Thermochimica Acta, 157 (1990) 181–191
Elsevier Science Publishers B.V., Amsterdam – Printed in The Netherlands

ON THE CRYSTALLIZATION KINETICS OF GLASSY ALLOYS IN THE Cu–As–Se SYSTEM

J. VÁZQUEZ, R.A. LIGERO, P. VILLARES and R. JIMÉNEZ-GARAY
Facultad de Ciencias, Universidad de Cádiz, Puerto Real (Spain)
(Received 12 June 1989)

ABSTRACT

A study of the crystallization kinetics of amorphous alloys in the Cu–As–Se system was made using a method in which the crystallization rate is deduced bearing in mind the dependence of the reaction rate constant on time, through temperature. The method was applied to the experimental data obtained by differential scanning calorimetry, using continuous-heating techniques. The kinetic parameters determined have made it possible to discuss the glass-forming ability, as well as the different types of nucleation and crystal growth exhibited by the alloys studied.

INTRODUCTION

The crystallization kinetics of glasses can be analysed using a wide variety of thermoanalytical techniques [1], each of which relies on a theoretical model [2] capable of partially describing the phenomenon involved. Owing to the complexity of the crystallization mechanisms, no one theory can be adopted which is capable of explaining the behaviour of any given glass as it crystallizes, and so all the methods that have been proposed have been subjected to comparative criticism [1], and even the mathematical developments on which they are based have been questioned [3].

Generally speaking, it is admitted that each type of amorphous material exhibits a behaviour which is most approximately described by one technique or another. For example, the crystallization of bulk chalcogenide glasses is considered to be adequately described by the Johnson–Mehl–Avrami theoretical model [2,4], to which different thermoanalytical techniques can be applied [2,5,6].

The alloys studied in this work, $Cu_xAs_{0.5-x}Se_{0.5}$, where $x = 0.05$ (M1), $x = 0.1$ (M2) and $x = 0.2$ (M3), are located in the centre of the area of homogeneous glasses corresponding to the composition diagram of the ternary system [7]. The crystallization kinetics of the alloys were analysed using differential scanning calorimetry (DSC), with continuous-heating methods.

0040-6031/90/$03.50

THEORY

The theoretical basis for the interpretation of the DSC results is provided by the formal theory of transformation kinetics, as developed by Johnson, Mehl and Avrami [8–10]. In its basic form, the theory describes the evolution over time of the crystallized fraction x in terms of the nucleation frequency per unit volume I_v and the crystalline growth rate u

$$x = 1 - \exp\left[-g \int_0^t I_v \left(\int_{t'}^t u \, d\tau \right)^m dt' \right] \tag{1}$$

where g is a geometric factor which depends on the shape of the crystalline growth and m is a parameter which depends on the mechanism of growth and the dimensionality of the crystal. For the important case of isothermal crystallization with time-independent nucleation and growth rates, eqn. (1) can be integrated to obtain

$$x = 1 - \exp(-g' I_v u^m t^n) \tag{2}$$

where $n = m + 1$ for $I_v \neq 0$ and g' is a new shape factor. Expression (2) can be identified with the Johnson–Mehl–Avrami relationship

$$x = 1 - \exp(-(Kt)^n) \tag{3}$$

in which K is defined as the reaction rate constant, which is usually assigned an Arrhenian temperature dependence

$$K = K_0 \, e^{-E/RT} \tag{4}$$

where E is the effective activation energy which describes the overall crystallization process and K_0 is the frequency factor. Comparison of eqns. (2) and (3) shows that K^n is proportional to $I_v u^m$ and, therefore, the consideration of an Arrhenian temperature dependence for K is only valid when I_v and u vary with temperature in an Arrhenian manner.

In general, nucleation frequency and crystalline growth rate exhibit far from Arrhenius-type behaviour [11,12]; however, for a sufficiently limited temperature range, such as the range of crystallization peaks in DSC experiments, both magnitudes can be considered to exhibit said behaviour.

It is a well-known fact that eqns. (3) and (4) are used as the basis of nearly all DTA and DSC crystallization experiments, but it must be noted that expression (3) can only be applied accurately in experiments carried out under isothermal conditions, for which it was deduced. However, this expression is often used for deducing relationships describing non-isothermal crystallization processes, because the values obtained for kinetic parameters are in good agreement with those determined through other methods. In spite of this, it is more accurate to integrate eqn. (1) under non-isothermal conditions and to consider that both I_v and u have an Arrhenian temperature dependence, resulting in an expression like eqn. (3), as proved by de

Bruijn et al. [13]. From this point of view, the crystallization rate is obtained by deriving expression (3) with respect to time, bearing in mind the fact that, in the non-isothermal process, the reaction rate constant is a time function through its Arrhenian temperature dependence [14], resulting in

$$\frac{dx}{dt} = n(Kt)^{n-1}\left[t\frac{dK}{dt} + K\right](1-x) \tag{5}$$

The maximum crystallization rate is found by making $d^2x/dt^2 = 0$, thus obtaining the relationship

$$(n-1)\left[t\frac{dK}{dt} + K\right]^2 + Kt\left[2\frac{dK}{dt} + t\frac{d^2K}{dt^2}\right] - n(Kt)^n\left[t\frac{dK}{dt} + K\right]^2 = 0 \tag{6}$$

in which by substituting dK/dt and d^2K/dt^2 for their expressions and introducing the heating rate $\beta = dT/dt$, we obtain the expression

$$\left(\frac{K_pT_p}{\beta}\right)^n = \frac{n-1+\left(\frac{E}{RT_p}\right)^2\Big/\left(1+\frac{E}{RT_p}\right)^{-2}}{n} \tag{7}$$

which relates the kinetic crystallization parameters E and n to the magnitude values (denoted by subscript p) that can be determined experimentally, and which correspond to the maximum crystallization rate.

Expression (7) has been specified for two interesting approximations as follows.

(i) The case where the activation energy E of the crystallization process is much less than RT_p, in which case it is verified that

$$y_p = -\ln(1-x_p) = \left(\frac{K_pT_p}{\beta}\right)^n \simeq \frac{n-1}{n} \tag{8}$$

which makes it possible to determine the reaction order n from the experimental value of the crystallized fraction x_p, corresponding to the maximum crystallization rate. By taking logarithms in eqn. (8) we obtain

$$\ln\frac{T_p}{\beta y_p^{1/n}} = \frac{E}{R}\frac{1}{T_p} - \ln K_0 \tag{9}$$

the equation of a straight line the slope of which gives the activation energy, and from the ordinate at the origin the frequency factor, K_0, is obtained.

(ii) If $E \gg RT_p$, the result obtained is

$$y_p = \left(\frac{K_pT_p}{\beta}\right)^n \simeq 1 \tag{10}$$

an expression from which it is deduced that the crystallized fraction for the maximum crystallization rate is 0.63, which, as may be observed, is indepen-

dent of the heating rate and the reaction order. The logarithmic form of eqn. (10) is

$$\ln \frac{T_p}{\beta} = \frac{E}{R} \frac{1}{T_p} - \ln K_0 \tag{11}$$

a linear relationship which makes it possible to calculate parameters E and K_0. At the same time, if the relationship $K_p T_p / \beta = 1$ is introduced into eqn. (5), we obtain

$$n = \frac{\left(\frac{dx}{dt}\right)_p RT_p}{0.37\, E\, K_p} \tag{12}$$

which makes it possible to calculate the reaction order or kinetic exponent n.

It should be noted that in non-isothermal crystallization experiments where the reaction rate constant may be considered to be temperature dependent according to the Arrhenius relationship, the aforementioned approximation is the most adequate, because in most crystallization reactions $E/RT_p \gg 1$ (usually $E/RT_p \geqslant 25$) [1].

EXPERIMENTAL

The alloys were made in bulk form, from their components of 99.99% purity which were pulverized to less than 64 μm, mixed in adequate proportions, and introduced into quartz ampoules. The ampoules were subjected to an alternating process of filling and vacuuming of inert gas, in order to ensure the absence of oxygen inside. This ended with a final vacuuming process of up to 10^{-5} Torr, and sealing with an oxyacetylene burner. The ampoules were put into a furnace at 950 °C for 3 h, turning at 1/3 r.p.m., in order to guarantee the homogeneity of the melted material, and then quenched in air to avoid crystallization.

The capsules containing the samples were then put into a mixture of hydrofluoridic acid and hydrogen peroxide in order to corrode the quartz and make it easier to extract the alloys.

The glassy nature of the materials was confirmed by X-ray diffractometric scanning, in a Siemens D-500 diffractometer, showing an absence of the peaks which are characteristic of crystalline phases. Figure 1 shows the corresponding diffractograms obtained with Mo $K\alpha$ radiation ($\lambda = 0.71069$ Å).

The calorimetric measurements were carried out in a Thermoflex DSC (Rigaku Corporation), to which an inert gas external installation was connected in order to ensure a constant He-55 flow of 60 cm^3 min^{-1}, to drag

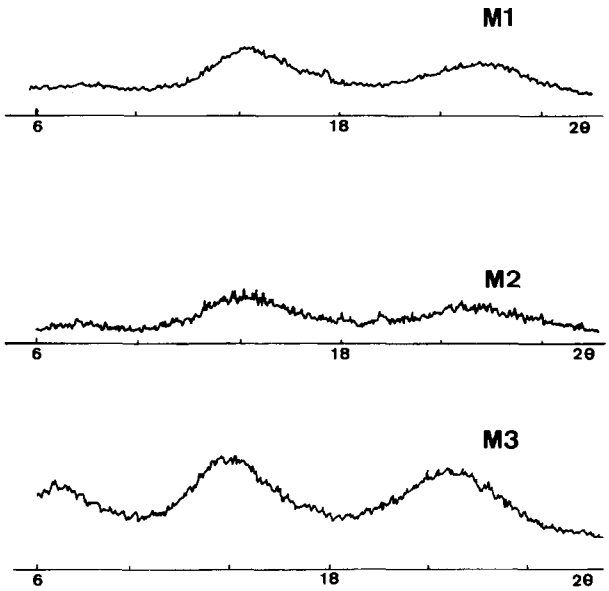

Fig. 1. Diffractograms of the three alloys M1–M3.

the gasses generated during the crystallization reactions, which, as is characteristic of chalcogenide materials, are very polluting for the DSC sensor equipment. The instrument was calibrated at the temperatures corresponding to the In, Sn and Pb melting points, and to a heating rate of 8 K min^{-1}.

The crystallizing experiments were carried out through continuous heating at rates β of 2, 4, 8, 16 and 32 K min^{-1}, and the masses used were kept within the range 12–26 mg. The pulverized samples were crimped (but not hermetically sealed) into aluminum pans, and empty aluminum pans were used as reference.

RESULTS AND DISCUSSION

The DSC registers give two crystallization peaks for alloy M1, one for M2 and three for M3, as shown in Fig. 2 with the registers corresponding to a heating rate of 16 K min^{-1}, for the three alloys. The two peaks shown for alloy M1 overlap for all values of β, and so it was not possible to resolve them by using any of the usual numerical techniques. It seemed more adequate to study their crystallization kinetics as a whole, as if it were only one crystallization peak.

The three exothermal peaks corresponding to alloy M3 also overlap, in general; however, it was possible to resolve them by using numerical analysis. The third peak is well defined for heating rates of 16 and 32 K min^{-1}. It is also observed that the second crystallization peak of this

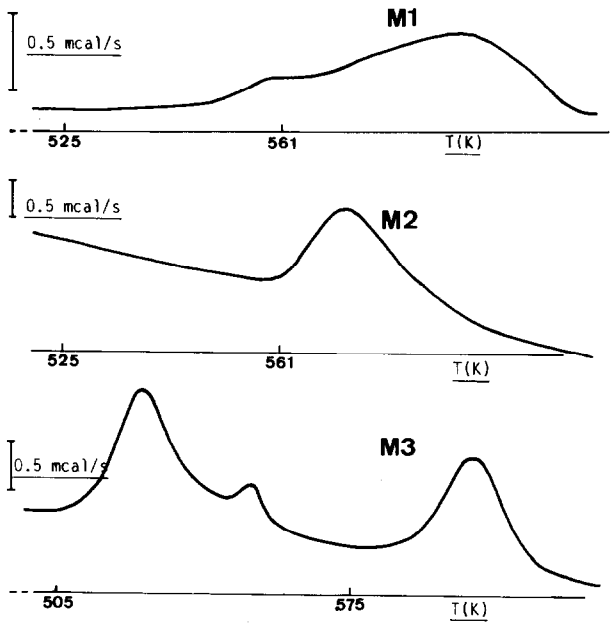

Fig. 2. Thermograms, at $\beta = 16$ K min^{-1}, for the three alloys M1–M3.

compound has an area equal to approximately 30% of each of the other two peaks, which have very similar areas.

The variation intervals of the magnitudes described by the thermograms, for different heating rates and for the three alloys are given in Table 1, where T_g is the glass transition temperature, T_{in} and T_p are the temperatures at which crystallization begins and that corresponding to the maximum crystallization rate, respectively, and ΔT is the width of the peak. The crystallization enthalpies ΔH were also determined, for the same heating rate at which the device was calibrated.

TABLE 1

The characteristic temperatures and enthalpies of the crystallization processes of alloys M1–M3

Parameter [a]	M1	M2	M3		
			Peak I	Peak II	Peak III
T_g (K)	449–466	453–469		446–464	
T_{in} (K)	533–561	543–565	491–505	523–537	539–587
T_p (K)	563–572	552–580	506–530	530–555	556–617
ΔT (K)	55– 80	20– 44	34– 48	12– 50	28– 60
ΔH (mcal mg^{-1})	11.06	3.79	10.69	3.83	11.07

[a] See text for definitions.

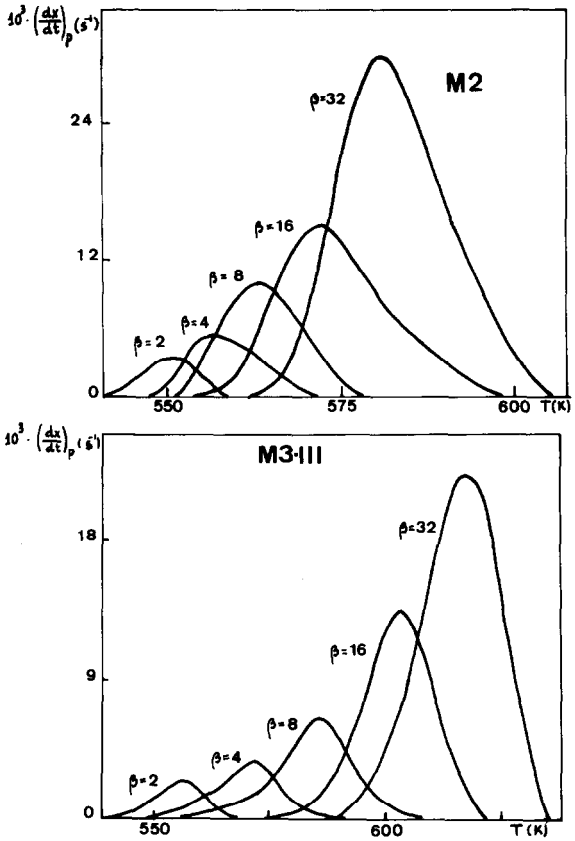

Fig. 3. Exothermal curves for M2 and the third stage of M3 for the crystallization peaks at heating rates of 2, 4, 8, 16 and 32 K min^{-1}.

The area under the DSC curve is directly proportional to the total amount of alloy crystallized. The ratio between the ordinates and the total area of the peak gives the corresponding crystallization rates, which makes it possible to build the curves of the exothermal peaks represented in Fig. 3, as an example, for alloy M2 and for the third peak of M3. It may be observed from Fig. 3 that the $(dx/dt)_p$ values increase in the same proportion as the heating rate, a property which has been widely discussed in the literature [15], and which is less evident in the case of hard-to-solve multiple peaks.

Bearing in mind that, in most crystallization processes, the activation energy is much larger than the product RT, the crystallization kinetics of the alloys in question were studied according to the appropriate approximation, described in the preceding theory. In alloy M1, it was observed that, immediately after completion of the crystallization process, the compound begins to melt. This is why the evaluation of the peak for high values of β is so uncertain that it seems advisable to ignore the experimental curve corresponding to $\beta = 32$ K min^{-1} when studying the crystallization kinetics of alloy M1.

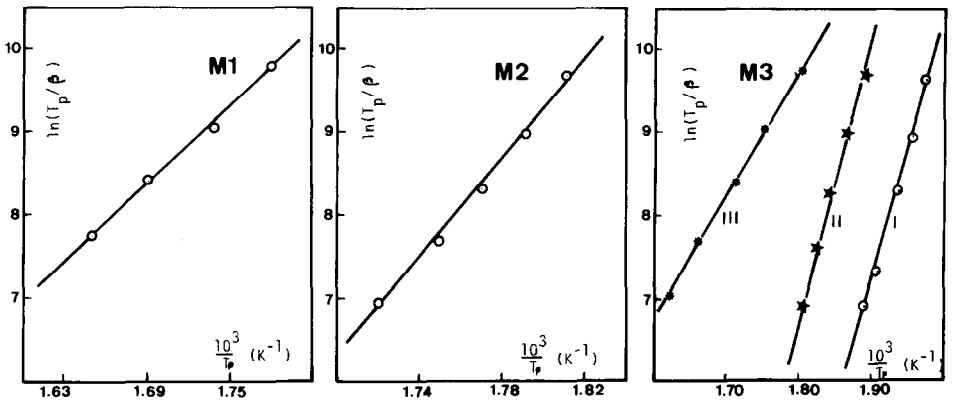

Fig. 4. Plots of $\ln(T_p/\beta)$ versus $1/T_p$ and straight regression lines for all the peaks of the alloys M1–M3.

The plots of $\ln(T_p/\beta)$ versus $1/T_p$ at each heating rate and for all the experimental peaks, and also the straight regression lines carried out are shown in Fig. 4. From the slope of these experimental straight lines, according to expression (11), it is possible to deduce the values of the activation energy, E, for the crystallization processes studied. In addition, the origin ordinate of these straight lines gives the values corresponding to the frequency factors K_0, which are given in Table 2 together with the activation energies.

By using the values of the frequency factor and the activation energy of the whole process, it is possible to calculate the value of the reaction rate constant, at each heating rate, which corresponds to the maximum crystallization rate. The results for both magnitudes are shown in Table 3. These values make it possible to determine, through relationship (12), the reaction order n of each process corresponding to each one of the experimental heating rates. This parameter is also shown in Table 3, where the rate constant corresponding to the maximum may also be observed to exhibit a similar behaviour for the crystallization rate peak values, in relation to the heating rates.

In agreement with the Avrami theory of nucleation, the mean values for the kinetic exponent show a two-dimensional growth for alloy M2, a

TABLE 2

The activation energies and frequency factors of alloys M1–M3

Parameter	M1	M2	M3		
			Peak I	Peak II	Peak III
E (kcal mol^{-1})	30.7	60.6	59.8	67.1	29.6
K_0 (s g^{-1})	6×10^{7}	7.7×10^{19}	6.2×10^{21}	3.2×10^{23}	2.7×10^{7}

TABLE 3

The maximum crystallization rates, corresponding rate constants and kinetic exponents for the different heating rates

Alloy	β (K min^{-1})	$(dx/dt)_p$ (s^{-1})	$10^3 K_p$ (s^{-1})	$10^3 \langle K_p \rangle$ (s^{-1})	n	$\langle n \rangle$
M1	2	0.00113	0.063	0.210	1.75	1.7
	4	0.00165	0.104		1.58	
	8	0.00342	0.241		1.46	
	16	0.00752	0.433		1.83	
	–	–	–		–	
M2	2	0.00342	0.065	0.366	2.6	2.0
	4	0.00531	0.118		2.2	
	8	0.00965	0.211		2.3	
	16	0.01443	0.464		1.6	
	32	0.02860	0.970		1.5	
M3 I	2	0.00249	0.071	0.402	1.6	1.3
	4	0.00342	0.130		1.2	
	8	0.00699	0.236		1.4	
	16	0.01378	0.478		1.3	
	32	0.02824	1.096		1.2	
II	2	0.00412	0.058	0.371	3.0	1.9
	4	0.00489	0.142		1.5	
	8	0.00875	0.247		1.5	
	16	0.02104	0.463		2.0	
	32	0.03005	0.945		1.4	
III	2	0.00265	0.058	0.339	4.5	3.6
	4	0.00394	0.121		3.4	
	8	0.00692	0.222		3.3	
	16	0.01444	0.475		3.3	
	32	0.02379	0.820		3.2	

one-dimensional growth for M1 and the first two peaks of M3, and a three-dimensional nucleation and growth process for the third stage of the latter [12,16,17].

Glass-forming ability (GFA) can be evaluated in terms of $\langle K_p \rangle$, as the meaning of the crystallization reaction rate constant [6,18]. In this sense it can be estimated that M2 and M3 have a similar GFA, although there is a decrease in this parameter as the copper concentration increases. This fact is also made evident by the values given in Table 2 for E and K_0, from which it may be observed that, for alloy M2 and the first two peaks of M3, the activation energies of the process are very similar, which means that the energy barrier which the glassy material must go through in order to attain the crystalline state is practically the same. On the other hand, the value of the frequency factors (which measure the probability of molecular collisions

effective for the formation of the activated complexes, in each case), are much greater for the aforementioned peaks of M3, thus implying a greater crystallizing ability for the compound containing more copper.

The similarity between the values deduced for kinetic parameters E and K_0, in alloy M1 and the third stage of M3, as well as the equality of the calculated enthalpies (Table 1), make it possible to expound the hypothesis that this peak of the latter alloy corresponds to a crystallization process of a phase which is analogous to that which crystallized in the case of alloy M1, i.e. the residual estechiometry of M3, after the first two crystallization processes, is of the same type as that originating the process in M1.

CONCLUSIONS

The alloys of the Cu–As–Se system exhibit multiple crystallization peaks, which shows the ability of Cu to form crystalline compounds, both binary and ternary, with the elements As and Se. In some of the alloys the crystallization peaks are so close together that they cannot be solved through the usual numerical techniques.

The method applied to the analysis of the crystallization kinetics of these alloys proved to be efficient and accurate, giving results which were in good agreement with the nature of the alloys under study, which are representative of different nucleation and crystalline-growth processes, according to the values found for the Avrami index.

The values obtained for the activation energies and the frequency factors make it possible to establish a criterion as to the GFA of these alloys, leading to the conclusion that, the greater the Cu concentration, the more difficult is the glass forming process in the system.

ACKNOWLEDGEMENTS

The authors are grateful to Aurora Rice for translating this paper into English, and to the Comisión Interministerial de Ciencia y Tecnología for their financial support (project no. MAT88-0561).

REFERENCES

1 H. Yinnon and D.R. Uhlmann, J. Non-Cryst. Sol., 54 (1983) 253.
2 S. Suriñach, M.D. Baro, M.T. Clavaquera-Mora and N. Clavaquera, J. Non-Cryst. Sol., 58 (1983) 209.
3 T. Kemeny and L. Granasy, J. Non-Cryst. Sol., 68 (1984) 193.
4 D.W. Henderson, J. Non-Cryst. Sol., 30 (1979) 301.

5 Yi Qun Gao and W. Wang, J. Non-Cryst. Sol., 81 (1986) 129.
6 R.A. Ligero, J. Vázquez, P. Villares and R. Jiménez-Garay, Mat. Lett., 8 (1989) 6.
7 Z.U. Borisova, Glassy Semiconductors, Plenum, New York, 1981.
8 W.A. Johnson and K.F. Mehl, Trans. Am. Inst. Mining Met. Eng., 135 (1981) 315.
9 M. Avrami, J. Chem. Phys., 7 (1939) 1103.
10 M. Avrami, J. Chem. Phys., 8 (1940) 212.
11 D. Turnball, Solid State Physics, Vol. 3, Academic Press, New York, 1956.
12 J.W. Christian, The Theory of Transformations in Metal and Alloys, 2nd edn., Pergamon, New York, 1975.
13 T.J.W. de Bruijn, W.A. de Jong and P.J. van der Berg, Thermochim. Acta, 45 (1981) 315.
14 J.A. Augis and J.E. Bennett, J. Thermal Anal., 13 (1978) 283.
15 Yi Qun Gao, W. Wang, F.Q. Zheng and X. Liu, J. Non-Cryst. Sol., 81 (1986) 135.
16 R. Chiba and N. Funakoshi, J. Non-Cryst. Sol., 105 (1988) 149.
17 S. Mahadevan, A. Giridhar and A.K. Singh, J. Non-Cryst. Sol., 88 (1986) 11.
18 H.E. Avery, Cinetica Química Básica y Mecanismos de Reacción, Reverté, Barcelona, 1977.